Facile preparation of a smart membrane with ammonia-responsive wettability transition for controllable oil/water…

Article *in* Journal of Materials Science · September 2017

DOI: 10.1007/s10853-017-1535-2

6 authors, including:

Yi He
Southwest Petroleum University
91 PUBLICATIONS **564** CITATIONS

SEE PROFILE

J Mater Sci (2017) 52:2169–2179

Facile fabrication of a robust superwetting three-dimensional (3D) nickel foam for oil/water separation

Xi Chen[2], Yi He[1,2,*], Yi Fan[2,*], Qiangbin Yang[2], Guangyong Zeng[2], and Heng Shi[2]

[1] *State Key Lab of Oil and Gas Reservoir Geology and Exploitation, Southwest Petroleum University, Rd. 8, Xindu District, Chengdu, Sichuan 610500, People's Republic of China*

[2] *School of Chemistry and Chemical Engineering, Southwest Petroleum University, Chengdu, Sichuan 610500, People's Republic of China*

Received: 22 August 2016
Accepted: 12 October 2016
Published online: 19 October 2016

ABSTRACT

A superwetting three-dimensional (3D) nickel foam was prepared by a facile electrodeposition process. Wettability, surface morphology, and chemical composition were characterized with contact angle test, scanning electron microscopy, Fourier transform infrared spectra, and X-ray photoelectron spectroscopy, respectively. According to the results, the as-prepared 3D nickel foam presented robust superhydrophobicity and superoleophilicity with good mechanical and chemical stability simultaneously. Furthermore, with the superwetting behavior, the nickel foam showed excellent oil/water separation capability with both high efficiency and lasting recyclability. Besides, the simple, low cost, and environmentally friendly fabrication process endows a scale-up of 3D nickel foam for oil/water separation and pollution disposal of leakage of organic solvents.

Introduction

In terms of the increasingly serious environmental pollution, such as oil spill accidents and industrial discharge of oily wastewaters, oil/water separation issue has become a hot research topic [1, 2]. Many studies have developed several approaches including coagulation, air flotation, oil skimmers, combustion, and oil containment booms [3–7] to solve these pollution problems. However, traditional approaches mentioned above have some defects containing low separation efficiency, expensive equipment, complicated procedure, and long processing time. It is imperative to find out a facile, low cost, significantly efficient, and environmentally friendly method in the separation of oil/water mixtures.

Biomimetic functional materials with superwetting behavior have drawn much concern both in academic researches and industrial applications. The lotus leaves are one of the most typical examples of superwetting materials, and the surface of lotus leaves has the ability of water repellency because of

Address correspondence to E-mail: chemheyi@swpu.edu.cn; tankvan5@gmail.com

DOI 10.1007/s10853-016-0505-4

the micro- and nano-structures and the hydrophobic wax-like compositions [8]. Inspired by lotus leaves, superhydrophobic materials have triggered various investigations due to their special properties, such as self-cleaning [9, 10], anticorrosion [11–13], microfluidic devices [14], antifogging [15, 16], and oil/water separation [17–21]. Generally, high surface roughness and low surface energy are indispensable for the fabrication of superhydrophobic surfaces [22, 23], from which researchers have developed various kinds of superhydrophobic surfaces. To address the shortcomings of traditional methods of oil/water separation, superhydrophobic and superoleophilic porous materials were employed as an improved way to separate oil from water [19, 24–28]. Separation of oil and water can be achieved with superhydrophobic and superoleophilic materials which can allow the selective penetration of oil while blocking the penetration of water simultaneously. Among the porous materials, three-dimensional (3D) porous structures were believed to have higher separation capacity and stronger adsorption kinetics than that of 2D meshes [29]. Therefore, nickel foam with 3D multilayer networks is considered to be beneficial for improving separation efficiency in oil/water separation and cleanup of oil spills. Furthermore, because of its toughness, thermal stability, and high mechanical performance, nickel foam is considered to be a promising substrate for building superwetting materials with long working life.

In the past years, various methods have been successfully employed to prepare the superhydrophobic and superoleophilic materials for oil/water separation, including sol–gel [30, 31], chemical vapor deposition [32, 33], electro-spinning [33, 34], chemical etching [35], self-assembly [19, 36], and so on. In order to develop a better way to realize oil/water separation and oil spills cleanup, a facile fabrication process is preferred. Besides, to the best of our knowledge, preparation of a superwetting nickel foam with separating function is less reported.

Herein, we employed a one-step electrodeposition method without any further surface modification to fabricate superhydrophobic and superoleophilic nickel foam (SS–NF) for oil/water separation and cleanup of oil spills. It is suitable for industrial application as it has some advantages such as simple operation, low toxicity, low cost, and convenience. Hence, it can be believed that the successful fabrication of superhydrophobic and superoleophilic nickel foam via the facile electrodepostion will have a great prospect in the field of oil/water separation.

Experiment

Materials

Stearic acid, nickel chloride hexahydrate, ethanol, sodium chloride, petroleum ether, toluene, and *N*-hexane were supplied by Kelong Chemical Reagent Co., Ltd. All of the reagents were of analytical grade. Deionized water with a resistance of 18.2 MΩ cm was provided by a UPC-III water purification system. Nickel foam (average pore diameter: 200 μm, pore number: 110 PPI) was obtained from Shenzhen greenid environmental protection filter Co. Ltd. Before the electrodeposition process, the nickel foam substrates were cut into pieces with different sizes, ultrasonically cleaned in acetone, and dried in air.

Electrodeposition process

Stearic acid and nickel chloride hexahydrate were added into ethanol under constant stirring until a uniform electrolyte solution was obtained. The direct-current power supply system (ZHAOXIN RXN-605D) was employed to two electrodes ranging from 5 to 60 V in electrolyte solution at room temperature, where the nickel foam acted as the cathode and platinum electrode was used as the anode. Finally, after a certain electrodeposition time, the sample was taken out, cleaned with ethanol, and dried in a vacuum oven at 60 °C for 20 min.

Characterization

The surface morphologies were characterized by Field-Emission Scanning Electron Microscope (FE-SEM, JSM-7500F). X-ray photoelectron spectroscopy (XPS, KRATOS XSAM 800 type, Al K ray) and FT-IR spectroscopy (WQF520) were employed to analyze chemical composition of the as-prepared nickel foam. The water contact angles and oil contact angles were measured using a contact angle meter (KRUSS DSA30S) with 5 μL droplets on specimens at ambient temperature. The average value was determined by measuring the same specimen at three different positions.

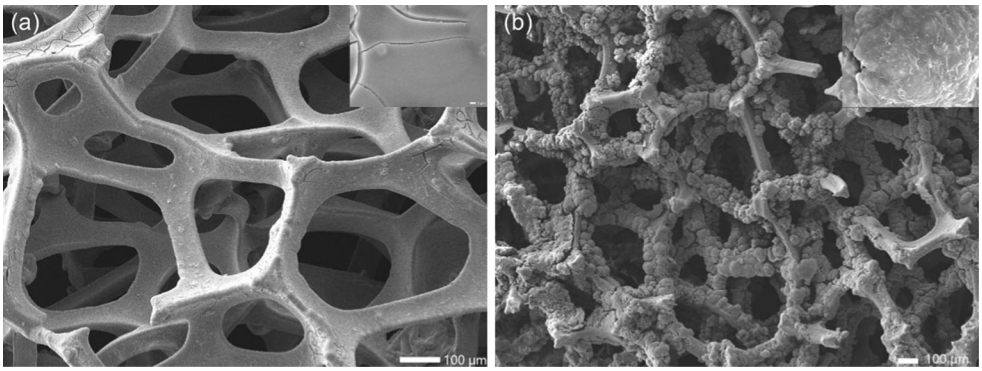

Figure 1 SEM images of **a** nickel foam and **b** SS–NF. *Insets* are enlarged drawing of the structure of nickel foam and SS–NF.

Mechanical abrasion test

The sample was stuck on a glass slide by adhesive, attached on glass slide weighing 100 g, and placed face down to the 400 grit sandpaper. We moved for 10 cm along the ruler, then the sample was rotated to 90° (face to the sandpaper), and moved for another 10 cm along the ruler [37]. This process is denoted as one cycle of the abrasion test, which guarantees that the surface is abraded to a larger extent in each cycle even if it is moved in a single direction.

The cycle experiment of oil/water separation

The cycle experiment is shown as follows. After the separation process was done, the nickel foam was washed with ethanol and dried in the vacuum oven at 60 °C. The as-dried nickel foam was used to repeat the process of oil/water separation.

Results and discussion

Morphology, chemical composition, and wettability

As Fig. 1a shows, the skeleton of the original nickel foam with porous structure is relatively smooth. On the contrary, from Fig. 1b we can observe that the skeleton of the SS–NF exhibits clear roughness and many packed micro/nano protrusions are formed. The hierarchical structure with high roughness makes air be easily trapped between these micro/nano protrusions, thus the actual contact area among surface and water droplet is decreased and the wettability is improved.

It is well-known that a combination of roughness structure and low surface energy leads to superhydrophobicity. Therefore, analysis of chemical composition of the SS–NF was made via FT-IR and XPS. The FT-IR spectra of pure stearic acid and SS–NF are presented in Fig. 2. The corresponding alkyl chain peaks can be seen at the same wavelength such as asymmetric vibration of $–CH_3$ (2956 cm^{-1}), asymmetric and symmetric vibrations of $–CH_2^-$ (2917, 2850 cm^{-1}) on both pure stearic acid and SS–NF. The peak for the carboxyl (−COO) group such as stretching vibration of C=O at 1701 cm^{-1} is disappeared on SS–NF. However, compared with FT-IR spectrum of stearic acid, SS–NF shows that a new peak appears at around 1540 and 1464 cm^{-1} [38, 39]. Consequently, we inferred that nickel stearate which provided low surface energy was deposited onto the foam surface. Figure 3 shows the XPS survey spectra of SS–NF. From the Fig. 3a, we can observe that Ni, O, and C are main components on the surface of samples. Besides, in C1s spectra of Fig. 3b, the peak at 284.6 eV is ascribed to methylene ($–CH_2^-$), and the peak at 288.4 eV is

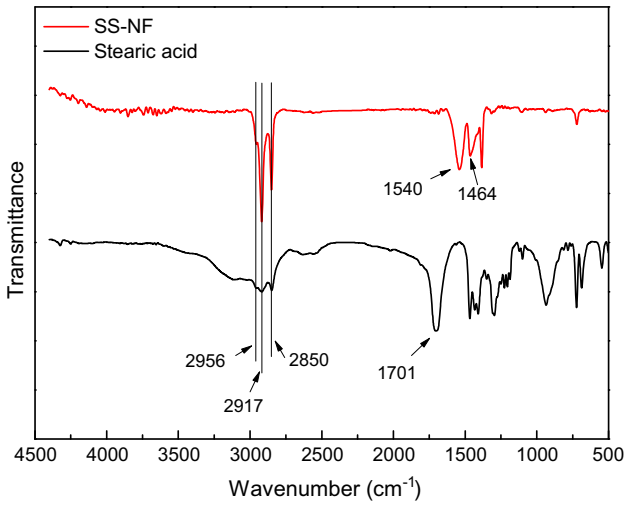

Figure 2 FT-IR spectra of pure stearic acid and SS–NF.

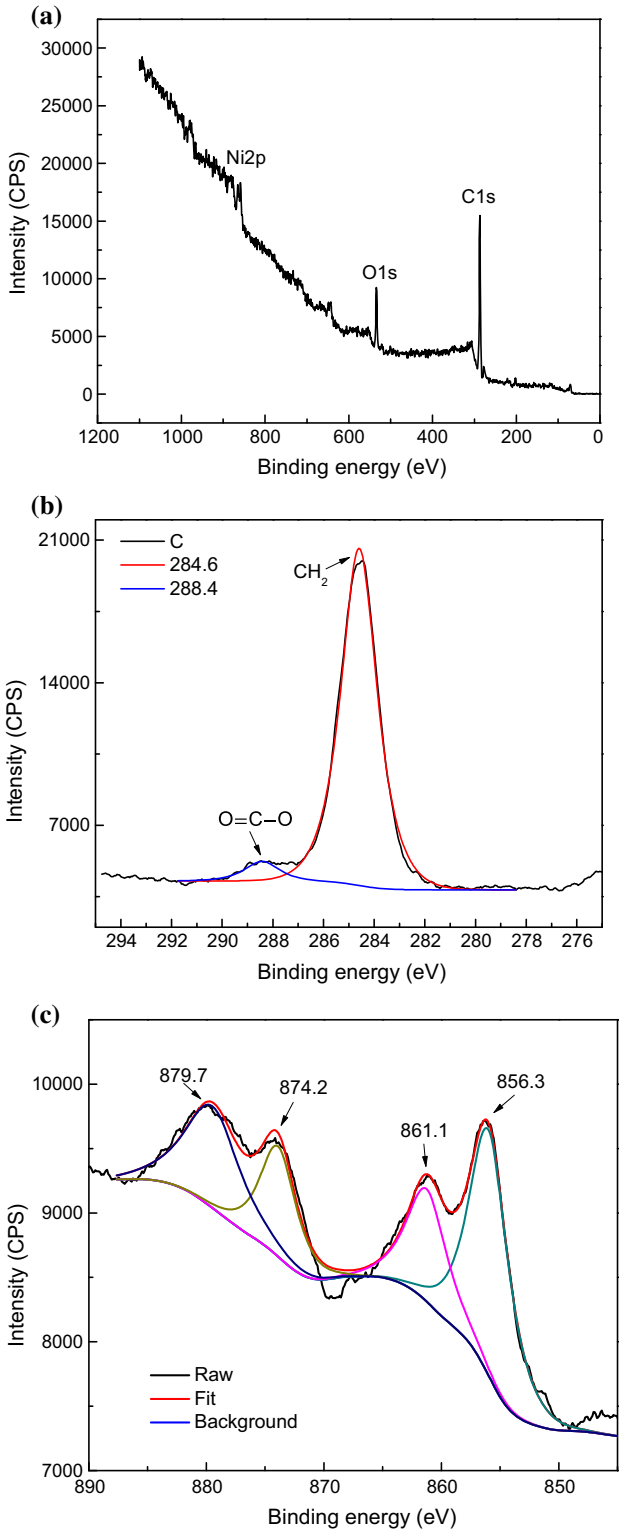

Figure 3 XPS spectra of the SS–NF: **a** survey spectrum, **b** C 1 s region, and **c** Ni 2p region.

attributed to carboxyl (−COO) group. In addition, the spectrum of Ni 2p presents two peaks at binding energies of 856.3 and 874.2 eV, which can be assigned to Ni $2p_{3/2}$ and Ni $2p_{1/2}$, respectively. And both peaks are accompanied by shake-up satellite features at 861.1 and 879.7 eV, respectively, indicating that the main valence state of Ni in the superhydrophobic layer is Ni^{2+} (II) [40, 41]. Therefore, these results demonstrate that the main composition of the superhydrophobic layer formed on nickel foam is nickel stearate ($Ni(CH_3(CH_2)_{16}COO)_2$).

Figure 4 shows the preparation process of SS–NF. When the constant voltage is applied to the electrodes, a part of stearic acid combines with free Ni^{2+} in the electrolyte solution to form nickel stearate and hydrogen ions (H^+). Meanwhile, some of the hydrogen ions (H^+) gain electrons to form H_2 with the electrodeposition proceeding. The reactions can be described as follows:

$$Ni^{2+} + 2CH_3(CH_2)_{16}COOH \rightarrow Ni\left(CH_3(CH_2)_{16}COO\right)_2 + 2H^+ \quad (1)$$

$$2H^+ + 2e^- \rightarrow H_2 \quad (2)$$

After this one-step electrodeposition process, the SS–NF was obtained.

Wettability of the SS–NF is shown in Fig. 5. The SS–NF exhibits superhydrophobicity with a water contact angle of 157° ± 0.3°. Meanwhile, the water droplet rolled off quickly from the surface of SS–NF in a slightly tilted angle about 1.8°. In sharp contrast, an oil droplet rapidly spread completely on the foam and the oil contact angle is almost 0° (Fig. 5b). According to the phenomena, it can be concluded that the as-prepared nickel foam is superhydrophobic and superoleophilic. To further determine the water-repellent ability of the SS–NF, a water droplet was forced to touch the surface and then lifted up. Figure 6 illustrates a dynamic water-adhesion test on the SS–NF. It can be seen that the water droplet departures completely from the surface without any residue even upon severe deformation, indicating that the nickel foam has an ultralow adhesion to water. The stable superhydrophobicity should be ascribed to the particles composed of nickel stearate. Consequently, a significant rough surface with low energy was made, and the excellent superhydrophobic

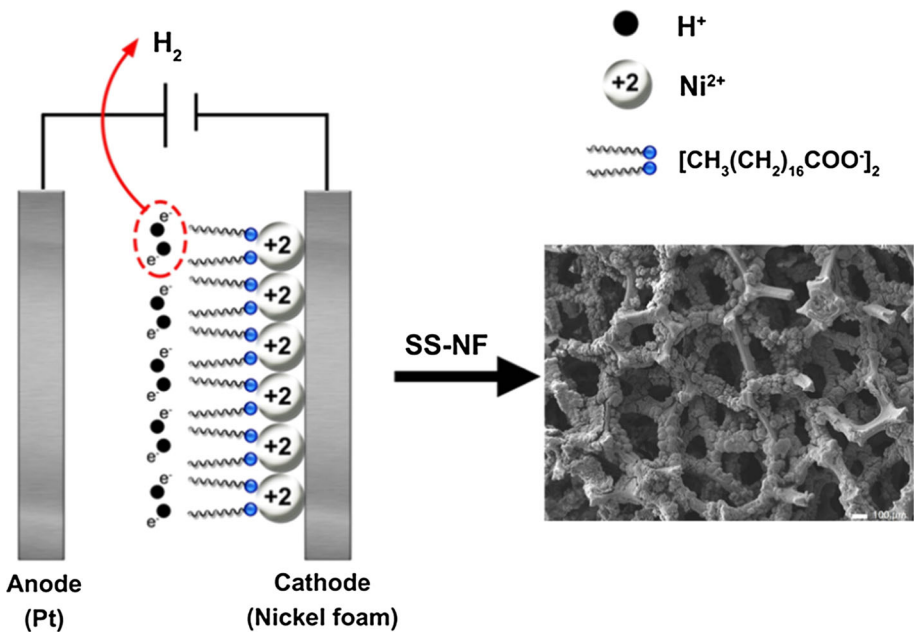

Figure 4 Schematic diagram of the preparation process of SS–NF.

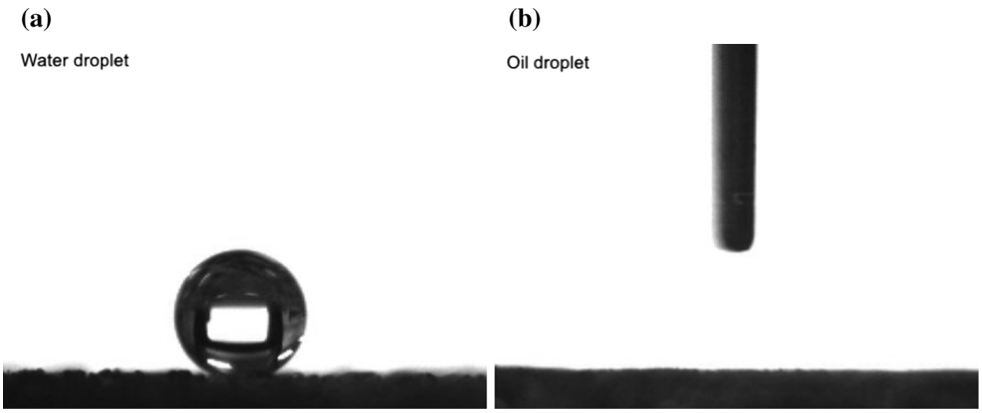

Figure 5 Optical images of **a** a water droplet with a contact angle of 157° ± 0.3°, **b** oil droplet (petroleum ether) with a contact angle of almost 0°.

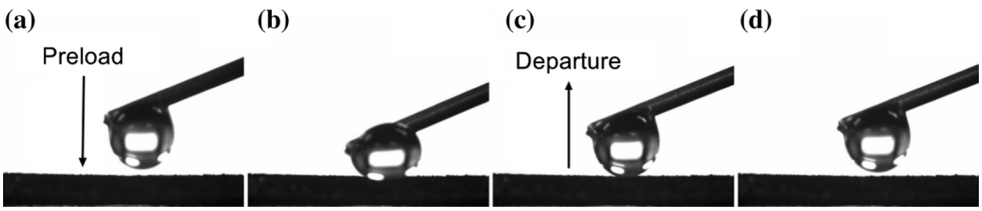

Figure 6 Dynamic water-adhesion measurement on the SS–NF.

nickel foam was obtained. As shown in Fig. 7, when the SS–NF was immersed in water, a silver bright surface was observed from the side. The phenomenon indicates that air could be trapped on the rough surface and a robust Cassie−Baxter state was built on the surface [42]. The Cassie−Baxter equation can be expressed as follows:

$$\cos\theta_r = f_1\cos\theta - f_2 \quad (3)$$

where f_1 and f_2 are the fractions of the solid surface and air in contact with the liquid, respectively, and θ_r and θ represent the water contact angles of the rough and smooth surfaces, respectively. The SS–NF surface can be idealized as a rough surface covered with

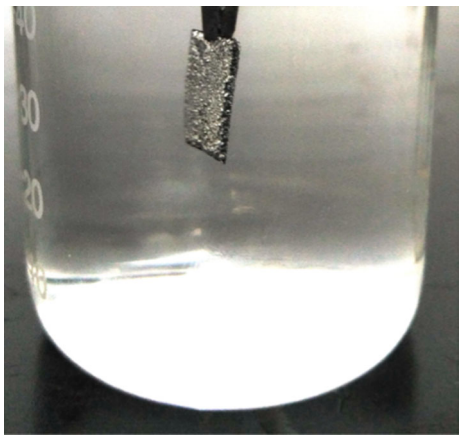

Figure 7 Digital graph of SS–NF immersed into water obtained with oblique angle.

–CH_3 group. Based on previous reports [43], water contact angle on the smooth surface with –CH_3 group is in a range of 113°–115°. Consequently, a large contact area fraction of air can greatly enhance hydrophobicity and the high roughness of SS–NF is the essential contributor to the superhydrophobic property.

The effects of electrodeposition parameters on wettability

We investigated the influences of the electrodeposition parameters on wetting condition. The effects of applied potential and electrodeposition time have been studied. Figure 8a presents the water contact angles and water sliding angles versus as a function of potential in 0.1 M stearic acid and 0.05 M nickel chloride ethanol solution at 10 min. From the image of Fig. 8a, the water contact angle is less than 150° with the electrodeposition voltage below 20 V. We further increased the applied potential to 20 V, and then the superhydrophobicity was achieved. Afterwards, we obtained the largest contact angle of 157° and the least sliding angle of 1.8° at the voltage of 40 V. Compared with 40 V, water contact and sliding angles had no obvious change when the potential was increased continuously. Consequently, we can deduce that high applied potential will promote the formation of this superhydrophobic surface to some extent.

Figure 8b shows the water contact and sliding angles changing as a function of treating time in 0.1 M stearic acid and 0.05 M nickel chloride ethanol solution at 40 V. Superhydrophobic sample can be

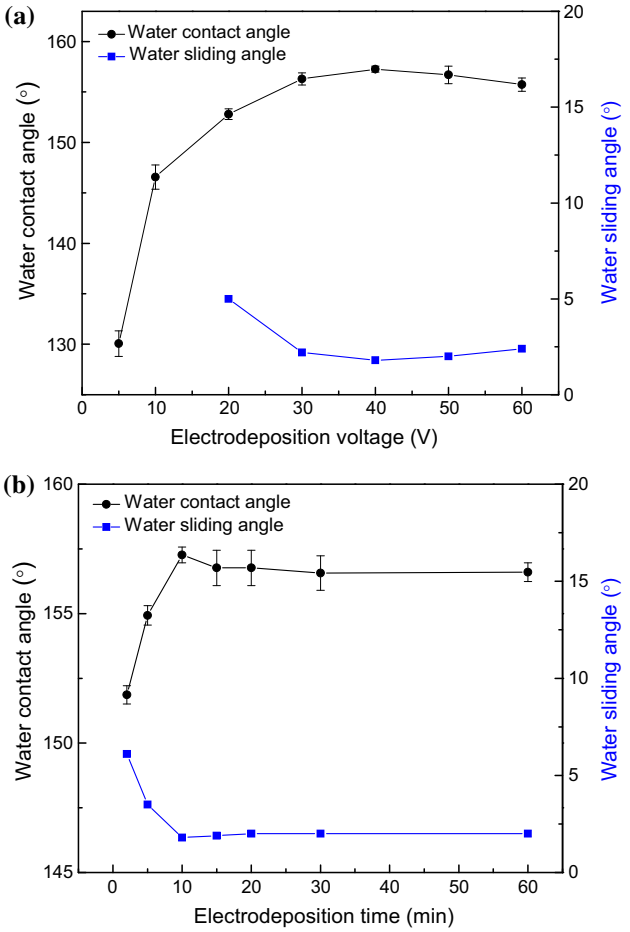

Figure 8 Variation in water contact angles and water sliding angles of the SS–NF as functions of **a** electrodeposition voltage, **b** electrodeposition time.

obtained after 2 min, implying that it's a faster way to fabricate superhydrophobicity. With 10 min, the extremum of contact and sliding angle was achieved, respectively. We further prolonged the electrodeposition time from 10 to 60 min, and there were few changes in water contact angle. The reason may be that the amount of nickel stearate is almost saturated within a short time about 10 min. It is noteworthy that water sliding angles of all the samples were less than 7°, revealing that an excellent superhydrophobicity was made under a deposition potential of 40 V.

Cleanup of oil spill and separation of water and oil

Nowadays, frequent oil spill accidents resulted in the pollution of sea ecosystems and coastal environments. It is necessary to remove and recycle oil spills from seawater efficiently. We expect that the SS–NF is

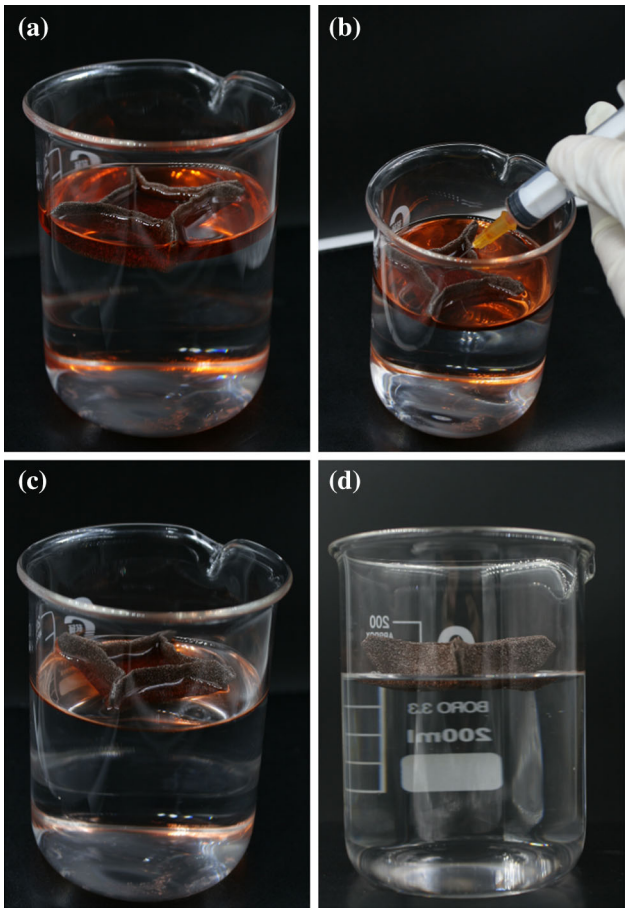

Figure 9 **a**–**d** Process of separating petroleum ether from water using SS–NF.

able to collect oil pollutants from water efficiently. So as to determine the collection capability of SS–NF, we designed a simulation test to remove oil spills from water as presented in Fig. 9. 20 mL petroleum ether dyed with Oil Red was added into a beaker including some water. As shown in Fig. 9a, owing to the superhydrophobicity and superoleophilicity, it can be seen that the SS–NF which was folded into a box can float on water and the petroleum ether can rapidly infiltrate into the box by gravitational effects while the water can be excluded. The petroleum ether in the box was transferred out continuously by syringe in Fig. 9b. After that, the residual petroleum ether continued to permeate into the box (Fig. 9c) until reaching a saturated value. Eventually, the petroleum ether on the water was almost disappearing as shown in Fig. 9d. The collected volume of petroleum ether is 18 mL, indicating that the collection capability of SS–NF is excellent. We hope that the SS–NF is a promising material without expensive production cost to cleanup and recycle oil spills efficiently.

In addition, it is also necessary to address the leakage of organic solvents with larger density than water in some industrial accident. Therefore, we also investigated the removal capability of SS–NF for dichloromethane under water. As shown in Fig. 10, the SS–NF rapidly adsorbed the dichloromethane (dyed with Oil Red) without any residual dichloromethane at the bottom of water, showing a good underwater adsorption performance.

Moreover, the SS–NF can be applied to oil/water separation due to its properties of superhydrophobicity and superoleophilicity. Diesel oil dyed with Oil Red and water was added into a beaker forming the oil and water mixture solution. Figure 11 exhibits that the SS–NF was placed in a beaker and the mixture solution of diesel oil and water was poured into the SS–NF. It can be observed that diesel oil rapidly spread on the sample and penetrated through the SS–NF. However, water was still excluded on the box and no water was noticed in the diesel oil layer. This phenomenon suggests that the separation ability of SS–NF is efficient. To further verify the separation ability of SS–NF, we also quantitatively investigated

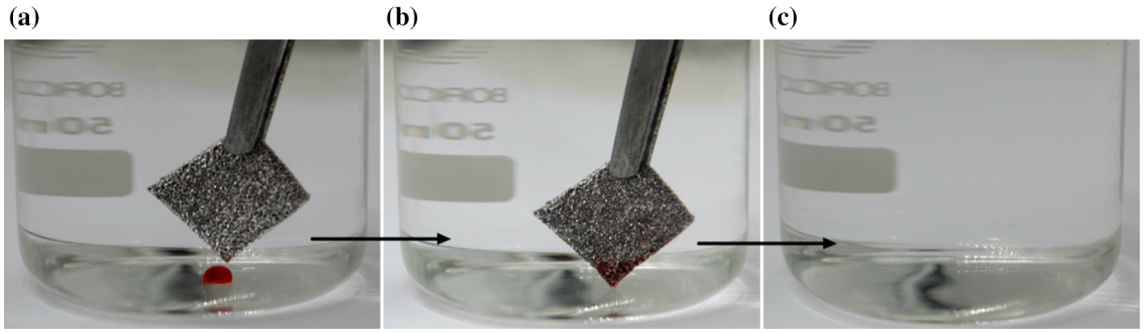

Figure 10 **a**–**c** Adsorption process of dichloromethane using SS–NF.

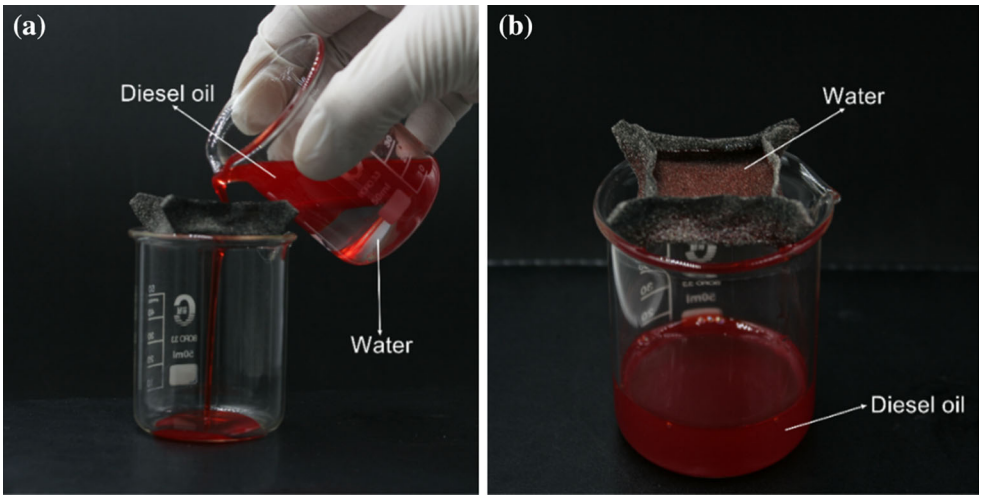

Figure 11 Separation process of the mixture of diesel oil and water.

the efficiency of SS–NF. The oil/water separation efficiency is defined as the mass ratio of the collected oil after separation process to the oil before separating. The separation efficiency of SS–NF for petroleum ether, toluene, diesel oil, and *N*-hexane is displayed in Fig. 12a. It can be seen that these types of oil were separated by the SS–NF at efficiency of more than 95 %. In addition, we also evaluated the recyclability and durability of the SS–NF. With the mixture of petroleum ether and water, the cycle experiments were carried out. As shown in Fig. 12b, the SS–NF still maintained a high separation efficiency (more than 94 %) even after ten cycles, demonstrating that the recyclability and durability of SS–NF was good. Furthermore, after washing and drying, water contact angle of the as-prepared sample was 152°, and the SS–NF still had superhydrophobic performance.

Mechanical stability and chemical stability

The weak mechanical stability of superhydrophobic materials greatly limits its practical application. Obviously, an excellent mechanical stability is an important index to evaluate the robustness of superhydrophobic materials for widespread applications. Nickel foam provides a good choice of substrate for fabricating robust superhydrophobic materials because of high mechanical performance. Figure 13 displays the schematic images of a mechanical abrasion test. As shown in Fig. 14, it can be seen that the water contact angles of SS–NF still maintained more than 150° after ten cycles of sandpaper abrasion tests. The contact angle of SS–NF

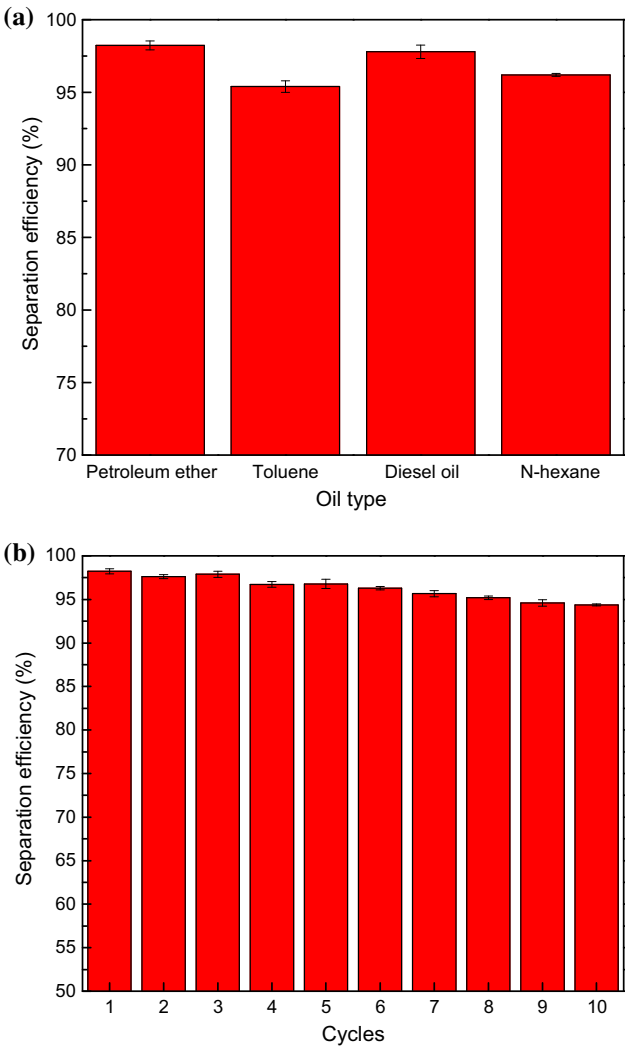

Figure 12 Separation efficiency of **a** different types of oil, **b** cycle experiments for petroleum ether.

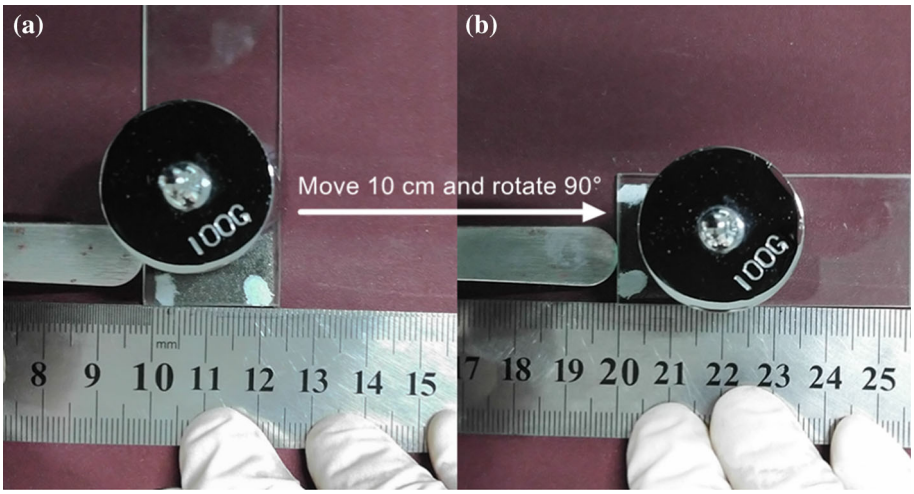

Figure 13 Schematic images of a mechanical abrasion test.

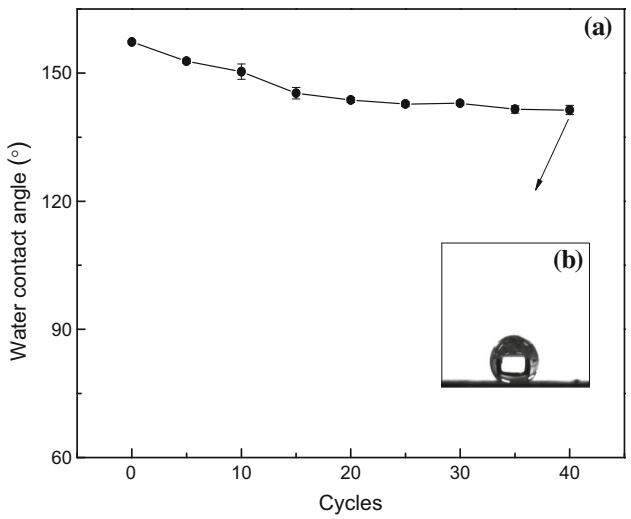

Figure 14 **a** Variation in water contact angles of the SS–NF as functions of the cycles of mechanical abrasion test. **b** Optical images of water droplet after 40 cycles of mechanical abrasion.

decreased to 145° after 15 cycles. However, there was no obvious further decreasing tendency in the subsequent cycles and the water contact angle was above 140° (Fig. 14b) after 40 cycles. In spite of that, SS–NF exhibits good mechanical abrasion resistance to some extent.

It is appreciated that the superhydrophobic materials will be applied in many harsh conditions such as high salinity, acidic, and basic environments. Therefore, it is very important for SS–NF to retain superhydrophobicity under such harsh environments. Water droplets with different pH values ranging from 1 to 13 were placed on the surface of SS–NF. As presented in Fig. 15a, there was no significant

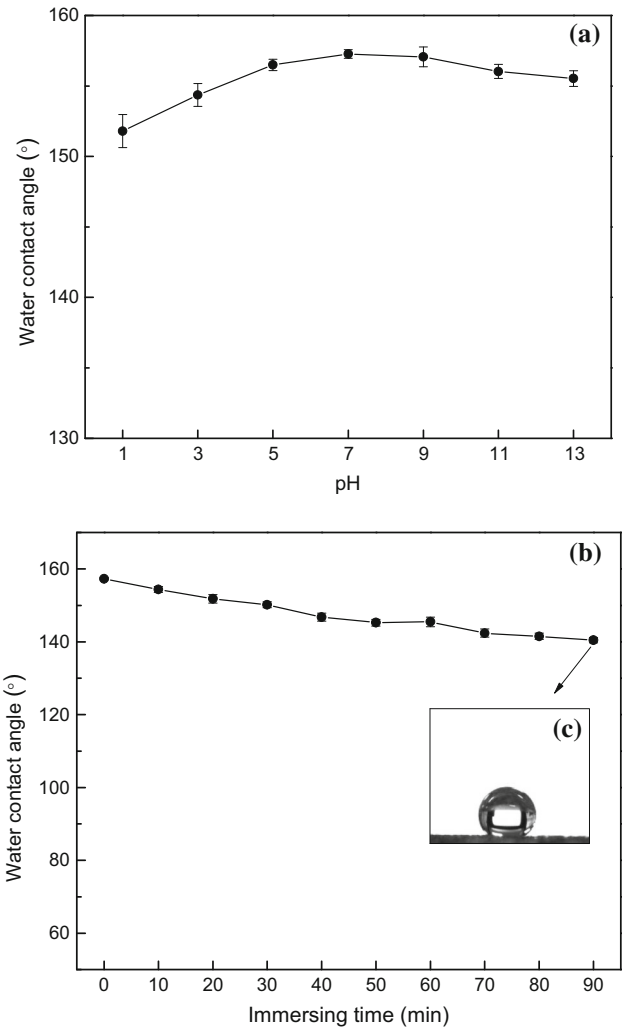

Figure 15 Change of water contact angles of the SS–NF as a function of **a** pH value, **b** immersing time, **c** Optical images of water droplet after immersing 90 min.

fluctuation of the contact angles which still maintained more than 150°. In order to further assess the chemical stability of SS–NF, the sample was immersed into 3.5 wt % NaCl solution at different times. Figure 15b displays the water contact angles versus immersing time in 3.5 wt % NaCl solution. It can be seen that the sample still kept superhydrophobicity after 30 min of immersion. Water contact angle decreased to 150° after 40 min, and the contact angles were still larger than 140° with the immersing time further extending to 90 min (Fig. 15c). All the results indicate that the SS–NF has a good chemical stability not only in aqueous solution of most acidic and alkali but also in some aqueous salts. A stable superhydrophobicity should be ascribed to the particles composed of nickel stearate.

Conclusion

We have developed a facile, low cost, and scalable electrodeposition process for fabricating the superwetting surface. The as-prepared nickel foam shows superhydrophobicity and superoleophilicity simultaneously. The treated nickel foam also presents excellent oil/water separation capability with both high efficiency and lasting recyclability. Besides, the as-prepared 3D nickel foam has good mechanical and chemical stability, which is critical for practical applications. The stable superhydrophobicity should be ascribed to the particles composed of nickel stearate. It is imagined that the superhydrophobic and superoleophilic 3D nickel foam has great potential for oil/water separation and cleanup of oil spills.

Acknowledgements

YH gratefully acknowledges Prof. H. Wang Analysis and Testing Center of Sichuan University for useful discussions and supports. The authors thank H. Wang for assistance with SEM measurements. This work was supported by the Youth science and technology creative group fund of Southwest Petroleum University (2015CXTD03).

References

[1] Shi H, He Y, Pan Y, Di H, Zeng G, Zhang L, Zhang C (2016) A modified mussel-inspired method to fabricate TiO_2 decorated superhydrophilic PVDF membrane for oil/water separation. J Membr Sci 506:60–70

[2] Yang X, He Y, Zeng G, Zhan Y, Pan Y, Shi H, Chen Q (2016) Novel hydrophilic PVDF ultrafiltration membranes based on a ZrO_2–multiwalled carbon nanotube hybrid for oil/water separation. J Mater Sci 51(19):8965–8976. doi:10.1007/s10853-016-0147-6

[3] Al-Shamrani A, James A, Xiao H (2002) Separation of oil from water by dissolved air flotation. Coll Surf A 209(1):15–26

[4] Mullin JV, Champ MA (2003) Introduction/overview to in situ burning of oil spills. Spill Sci Technol Bull 8(4):323–330

[5] Ventikos NP, Vergetis E, Psaraftis HN, Triantafyllou G (2004) A high-level synthesis of oil spill response equipment and countermeasures. J Hazard Mater 107(1):51–58

[6] Wong K-FV, Barin E (2003) Oil spill containment by a flexible boom system. Spill Sci Technol Bull 8(5):509–520

[7] Zouboulis A, Avranas A (2000) Treatment of oil-in-water emulsions by coagulation and dissolved-air flotation. Coll Surf A 172(1):153–161

[8] Barthlott W, Neinhuis C (1997) Purity of the sacred lotus, or escape from contamination in biological surfaces. Planta 202(1):1–8

[9] Blossey R (2003) Self-cleaning surfaces—virtual realities. Nat Mater 2(5):301–306

[10] Deng X, Mammen L, Butt H-J, Vollmer D (2012) Candle soot as a template for a transparent robust superamphiphobic coating. Science 335(6064):67–70

[11] Liu Y, Li S, Zhang J, Liu J, Han Z, Ren L (2015) Corrosion inhibition of biomimetic super-hydrophobic electrodeposition coatings on copper substrate. Corros Sci 94:190–196

[12] Fan Y, He Y, Luo P, Chen X, Liu B (2016) A facile electrodeposition process to fabricate corrosion-resistant superhydrophobic surface on carbon steel. Appl Surf Sci 368:435–442

[13] Liu Q, Chen D, Kang Z (2015) One-step electrodeposition process to fabricate corrosion-resistant superhydrophobic surface on magnesium alloy. ACS Appl Mater Interfaces 7(3):1859–1867

[14] Sousa MP, Mano JF (2013) Patterned superhydrophobic paper for microfluidic devices obtained by writing and printing. Cellulose 20(5):2185–2190

[15] Sun Z, Liao T, Liu K, Jiang L, Kim JH, Dou SX (2014) Fly-eye inspired superhydrophobic anti-fogging inorganic nanostructures. Small 10(15):3001–3006

[16] Yao L, He J (2014) Broadband antireflective superhydrophilic thin films with outstanding mechanical stability on glass substrates. Chin J Chem 32(6):507–512

[17] Wang B, Guo Z (2013) Superhydrophobic copper mesh films with rapid oil/water separation properties by electrochemical

deposition inspired from butterfly wing. Appl Phys Lett 103(6):063704

[18] Yu Y, Chen H, Liu Y, Craig V, Li LH, Chen Y (2014) Superhydrophobic and superoleophilic boron nitride nanotube-coated stainless steel meshes for oil and water separation. Adv Mater Interfaces 1(1):1300002

[19] Wu C, Huang X, Wu X, Qian R, Jiang P (2013) Mechanically flexible and multifunctional polymer-based graphene foams for elastic conductors and oil-water separators. Adv Mater 25(39):5658–5662

[20] Zhang J, Ji K, Chen J, Ding Y, Dai Z (2015) A three-dimensional porous metal foam with selective-wettability for oil–water separation. J Mater Sci 50(16):5371–5377. doi:10.1007/s10853-015-9057-2

[21] Wang E, Wang H, Liu Z, Yuan R, Zhu Y (2015) One-step fabrication of a nickel foam-based superhydrophobic and superoleophilic box for continuous oil–water separation. J Mater Sci 50(13):4707–4716. doi:10.1007/s10853-015-9021-1

[22] Feng X, Feng L, Jin M, Zhai J, Jiang L, Zhu D (2004) Reversible super-hydrophobicity to super-hydrophilicity transition of aligned ZnO nanorod films. J Am Chem Soc 126(1):62–63

[23] Sun T, Wang G, Feng L, Liu B, Ma Y, Jiang L, Zhu D (2004) Reversible switching between superhydrophilicity and superhydrophobicity. Angew Chem Int Ed 43(3):357–360

[24] Kong L-H, Chen X-H, Yu L-G, Wu Z-S, Zhang P-Y (2015) Superhydrophobic cuprous oxide nanostructures on phosphor-copper meshes and their oil–water separation and oil spill cleanup. ACS Appl Mater Interfaces 7(4):2616–2625

[25] Lu Y, Sathasivam S, Song J, Chen F, Xu W, Carmalt CJ, Parkin IP (2014) Creating superhydrophobic mild steel surfaces for water proofing and oil–water separation. J Mater Chem A 2(30):11628–11634

[26] Song J, Huang S, Lu Y, Bu X, Mates JE, Ghosh A, Ganguly R, Carmalt CJ, Parkin IP, Xu W (2014) Self-driven one-step oil removal from oil spill on water via selective-wettability steel mesh. ACS Appl Mater Interfaces 6(22):19858–19865

[27] Yang Y, Liu Z, Huang J, Wang C (2015) Multifunctional, robust sponges by a simple adsorption–combustion method. J Mater Chem A 3(11):5875–5881

[28] Zhang X, Li Z, Liu K, Jiang L (2013) Bioinspired multifunctional foam with self-cleaning and oil/water separation. Adv Funct Mater 23(22):2881–2886

[29] Zang D, Wu C, Zhu R, Zhang W, Yu X, Zhang Y (2013) Porous copper surfaces with improved superhydrophobicity under oil and their application in oil separation and capture from water. Chem Commun 49(75):8410–8412

[30] Leventis N, Chidambareswarapattar C, Bang A, Sotiriou-Leventis C (2014) Cocoon-in-web-like superhydrophobic aerogels from hydrophilic polyurea and use in environmental remediation. ACS Appl Mater Interfaces 6(9):6872–6882

[31] Li R, Chen C, Li J, Xu L, Xiao G, Yan D (2014) A facile approach to superhydrophobic and superoleophilic graphene/polymer aerogels. J Mater Chem A 2(9):3057–3064

[32] Zhang J, Seeger S (2011) Polyester materials with superwetting silicone nanofilaments for oil/water separation and selective oil absorption. Adv Funct Mater 21(24):4699–4704

[33] Zhou X, Zhang Z, Xu X, Men X, Zhu X (2013) Facile fabrication of superhydrophobic sponge with selective absorption and collection of oil from water. Ind Eng Chem Res 52(27):9411–9416

[34] Wang L, Yang S, Wang J, Wang C, Chen L (2011) Fabrication of superhydrophobic TPU film for oil–water separation based on electro spinning route. Mater Lett 65(5):869–872

[35] Guo W, Zhang Q, Xiao H, Xu J, Li Q, Pan X, Huang Z (2014) Cu mesh's super-hydrophobic and oleophobic properties with variations in gravitational pressure and surface components for oil/water separation applications. Appl Surf Sci 314:408–414

[36] Wang L, Pan K, Li L, Cao B (2014) Surface hydrophilicity and structure of hydrophilic modified PVDF membrane by nonsolvent induced phase separation and their effect on oil/water separation performance. Ind Eng Chem Res 53(15):6401–6408

[37] Lu Y, Sathasivam S, Song J, Crick CR, Carmalt CJ, Parkin IP (2015) Robust self-cleaning surfaces that function when exposed to either air or oil. Science 347(6226):1132–1135

[38] Wang P, Zhang D, Lu Z (2015) Advantage of super-hydrophobic surface as a barrier against atmospheric corrosion induced by salt deliquescence. Corros Sci 90:23–32

[39] Liu T, Chen S, Cheng S, Tian J, Chang X, Yin Y (2007) Corrosion behavior of super-hydrophobic surface on copper in seawater. Electrochim Acta 52(28):8003–8007

[40] Yoshida T, Yamasaki K (1981) The core-level binding energies and the structures of nickel complexes. Bull Chem Soc Jpn 54(3):935–936

[41] Matienzo J, Yin LI, Grim SO, Swartz WE Jr (1973) X-ray photoelectron spectroscopy of nickel compounds. Inorg Chem 12(12):2762–2769

[42] Wang P, Zhang D, Qiu R, Wu J (2014) Super-hydrophobic metal-complex film fabricated electrochemically on copper as a barrier to corrosive medium. Corros Sci 83:317–326

[43] Cui Z, Wang Q, Xiao Y, Su C, Chen Q (2008) The stability of superhydrophobic surfaces tested by high speed current scouring. Appl Surf Sci 254(10):2911–2916